STUDY OF IRREGULAR WAVE-CURRENT-MUD INTERACTION

Mohsen Soltanpour[1], Farzin Samsami[2], Tomoya Shibayama[3] and Sho Yamao[4]

The dissipation of regular and irregular waves on a muddy bed with the existence of following and opposing currents are investigated through a series of wave flume laboratory experiments. The commercial kaolinite is used as fluid mud layer. The laboratory results show the increase of both regular and irregular wave heights due to opposing currents. On the other hand, the following currents result to the decrease of the wave heights. In the numerical treatment, the deformation of wave due to current was first calculated based on the conservation equation of wave action and then the attenuation of this deformed wave due to the muddy bed is simulated by a multi-layered wave-mud interaction model. Acceptable agreements were observed between the numerical results and laboratory data.

Keywords: Wave-current interaction; irregular wave; fluid mud; wave dissipation; wave flume experiments

INTRODUCTION

Waves and current interaction is a complex phenomenon in coastal and estuarine areas. Longuet-Higgins and Stewart (1961) used the radiation stress concept to find out solutions for wave-current interaction and examined the energy transfer between waves and currents. They proposed an equation to determine the wave height variation for steady currents and no energy loss condition. The other early research was developed by Bretherton and Garrett (1968). Instead of employing energy equation, the wave action equation (i.e. wave energy density/wave frequency relative to the current) was derived in their theory to simplify the wave-current interaction. The later theory has given a good prediction on the wave height variation and it is a simple solution to be adopted in the coastal processes.

The effect of wave-current field on a muddy bed is of considerable practical interests too. However, literature shows few studies on wave-current-mud interaction. An and shibayama (1994) performed a series of wave flume experiments of regular wave-current interaction on fluid mud layer. Their results indicated higher values of wave dissipation rates and mud mass transport velocities due to existence of opposing currents. In the other study by De Wit and Kranenburg (1996), experimental studies of wave-fluid mud interaction with the presence of a net current were examined in a wave-current flume using two artificial mud. Modifying Gade's model (1958), they found a well agreement in comparison between the measured and calculated wave attenuation rates and wave-induced velocities. Zhao et al. (2006) performed numerical and experimental studies on wave-current-mud interaction. They proposed a numerical model based on an eddy viscosity model for wave and current interaction and then coupled the motion equation with mud layer. Soltanpour et al. (2008) proposed a numerical wave-mud-current interaction model to simulate wave transformation and mud mass transport with presence of a uniform current using the conservation equation of wave action by Thomas (1981). They also compared the results of their numerical model with the laboratory data of An and Shibayama (1994). Kaihatu and Tahvildari (2012) proposed a frequency-domain model to investigate the combination effects of wave nonlinearity, mud-induced dissipation and wave-current interaction. The calculated dissipation rates were compared with the laboratory data of An and Shibayama (1995) and Zhao et al. (2006). The propagation of cnoidal waves on muddy bed under the opposing and following currents was also investigated in their modeling study.

A series of wave flume experiments was conducted in this study to investigate the attenuation of waves along soft mud layers with the presence of currents. Both regular waves and irregular waves with two different wave spectra, i.e., JONSWAP and Bretschneider, were employed. The conservation equation of wave action was employed to model the deformation of incident wave due to current. The wave attenuation is then computed using the numerical multi-layered wave-mud interaction model of Soltanpour et al. (2007).

[1] Civil Engineering Department, K. N. Toosi University of Technology, Vali-Asr St., Tehran, Iran
[2] Formerly, Civil Engineering Department, K. N. Toosi University of Technology, Vali-Asr St., Tehran, Iran
[3] Civil & Environmental Engineering Department, Waseda University, Tokyo, Japan
[4] Civil & Environmental Engineering Department, Waseda University, Tokyo, Japan

MODELING OF WAVE-CURRENT-MUD INTERACTION

Regular Wave-Current Interaction

The first attempt to deal with the wave propagation over non-uniform current was proposed by Longuet-Higgins and Stewart (1961). They introduced the term of "Radiation Stress" based on steady and no energy loss condition as follows

$$\nabla.[E(C_{gr}+U)]+S_{ij}\gamma_{ij}=0 \tag{1}$$

where E is the energy density, C_{gr} is group velocity, U is current velocity, S_{ij} is radiation stress tensor and γ_{ij} is the rate of strain tensor associated with the current. In another simple treatment, Bretherton and Garrett (1968) used the wave action, i.e. wave energy density divided by wave frequency relative to the current, to study the wave-current interaction. The wave action equation can be written as

$$\frac{\partial}{\partial t}(\frac{E}{\sigma_r})+\nabla.[\frac{E}{\sigma_r}(C_{gr}+U)]=0 \tag{2}$$

where σ_r is the relative angular frequency defined by $\sigma_r=\omega-kU$, ω is angular frequency, U is the mean depth-averaged current velocity and k is wave number. The radiation stress and wave action equations are identical for steady state. Many researchers followed these two theories to investigate different aspects of regular wave-current interaction (e.g., Whitham 1962; Dalrymple 1974; Peregrine 1976; Brevik and Aas 1980; Thomas 1981).

Following Thomas (1981), the deformed wave height and wavelength can be predicted under the steady condition and the wave action equation as:

$$\frac{E}{\sigma_r}(C_{gr}+U)=Const. \tag{3}$$

or

$$\frac{H^2}{\sigma_r}(C_{gr}+U)=Const. \tag{4}$$

Considering the irrotational dispersion equation

$$\sigma_r^{\,2}-gk\tanh kd=0 \tag{5}$$

$$(\omega-kU)^2-gk\tanh kd=0 \tag{6}$$

where d is water depth. In order to define the constant value, it is necessary to specify a reference level as no current condition. Newton-Raphson method is used in numerical calculation to find out the wave height variations under current condition.

Spectral Wave-Current Interaction

In a simple treatment, the more complicated changes in wave spectra caused by current can be obtained following the equation proposed by Huang et al. (1972) as

$$\frac{\partial}{\partial x}[\frac{E(C_{gr}+U)}{\omega_r}]=0 \tag{7}$$

where ω_r is angular wave frequency in frame of reference moving with current (intrinsic angular wave frequency). As wave propagates from no current condition to a current one, Eq. (7) can be rewritten as

$$\frac{E_0C_{g0}}{\omega_a}=\frac{E(C_{gr}+U)}{\omega_r} \tag{8}$$

where the subscript "0" refers to no current condition and ω_a is angular wave frequency in stationary frame of reference (apparent angular wave frequency). Considering the linear wave theory, the group velocities are defined as

$$C_{g0} = \frac{1}{2}(1+\frac{2k_0 d}{\sinh 2k_0 d})\frac{\omega_a}{k_0} \tag{9}$$

$$C_{gr} = \frac{1}{2}(1+\frac{2kd}{\sinh 2kd})\frac{\omega_r}{k} \tag{10}$$

The spectral density in this transition condition can be written as follows

$$\frac{S_{\eta\eta}(\omega_a,U)}{S_{\eta\eta}(\omega_a)}\left[=\frac{S_{\eta\eta}(\omega_a,U)d\omega_a}{S_{\eta\eta}(\omega_a)d\omega_a}=\frac{E}{E_0}\right]=\frac{\omega_r\left[1+\left(\frac{2k_0 d}{\sinh 2k_0 d}\right)\right]}{2k_0\left\{U+\left[1+\left(\frac{2kd}{\sinh 2kd}\right)\right]\frac{\omega_r}{2k}\right\}} \tag{11}$$

Assuming that the waves are not refracted by current and water depth is sufficiently deep, the deformed wave spectrum will be

$$\frac{S_{\eta\eta}(\omega_a,U)}{S_{\eta\eta}(\omega_a)}=\frac{\omega_r^2}{\omega_a^2}\frac{1}{\left(1+\frac{2U\omega_r}{g}\right)}=\frac{1}{\left(1+\frac{U\omega_r}{g}\right)^2\left(1+\frac{2U\omega_r}{g}\right)}=\frac{4}{\left[1+\left(1+\frac{4U\omega_a}{g}\right)^{1/2}\right]^2\left(1+\frac{4U\omega_a}{g}\right)^{1/2}} \tag{12}$$

Simulation of wave-current interaction on fluid mud

In spite of considerable practical applications, there has been few studies on wave-current-mud interaction (e.g., Zhao and Li 1994; An and Shibayama 1994; Zhao et al. 2006; Soltanpour et al. 2008). It is assumed here that the wave attenuation process will take place after regular/irregular waves are deformed due to the currents. The theory of Thomas (1981) is followed to calculate the change of regular wave.

For the case of a spectral wave, the deformed wave spectrum due to current action is first calculated based on Huang et al. (1972). Employing Fourier theory, the spectral wave is then presented as superposition of many simple, regular harmonic wave components having their own amplitudes and periods. The numerical model of Soltanpour et al. (2007) is used for the calculation of attenuation of both regular waves and harmonic components of spectral waves.

EXPERIMENTAL INVESTIGATIONS

Wave flume experiments were performed in Coastal Engineering Laboratory of Department of Civil and Environmental Engineering at Waseda University, Japan. The glass-sided flume has a cross section of 40.5 cm wide by 60 cm deep in cross-section and the total length of 13.8 m. Irregular waves were generated by a flap-type wavemaker. Following and opposing currents can be generated by a pump system through an inlet or outlet located at the bottom of flume. Three capacitance wave gauges were employed to measure wave heights while the current velocity was recorded by an electro-magnetic current meter in a fixed location about 12cm above the muddy bed. The data of gauge 2 presents the measured deformed irregular wave due to current and gauge 3 shows the wave under both effects of current and fluid mud. Two false beds were placed in the flume to confine the 2m long mud section with a thickness of 10 cm. Fig. 1 shows the sketch of experimental setup.

A well mixture of commercial kaolinite with tap water was used as muddy bed. The chemical characteristics of the used kaolinite were SiO_2=45.9%, Al_2O_3=37.8% and Fe_2O_3=0.6%; and the particle size distribution follows D_{40} and D_{86} of 2 μm and 10 μm, respectively. The rheological behavior of kaolinite was tested with an Anton Paar Physica MCR300 instrument at the Rheometry Laboratory of Institute for Colorants, Paint, and Coatings (ICPC). This instrument allows any type or combination of rheological tests, both in rotational and oscillatory modes. Viscoelastic characteristics of the fluid mud were measured using the oscillatory frequency sweep test. Applying the least square method to the data, Fig. 2 represents the Kelvin-Voigt viscoelastic parameters μ and G for the used kaolinite where W is the water content ratio of the mud sample (%). It is observed that viscoelastic parameters depend not only on the water content ratio of the mud but also strongly on the frequency. Table 1 lists the fitted parameters of G (Pa) and μ (Pa.s) to the rheological tests.

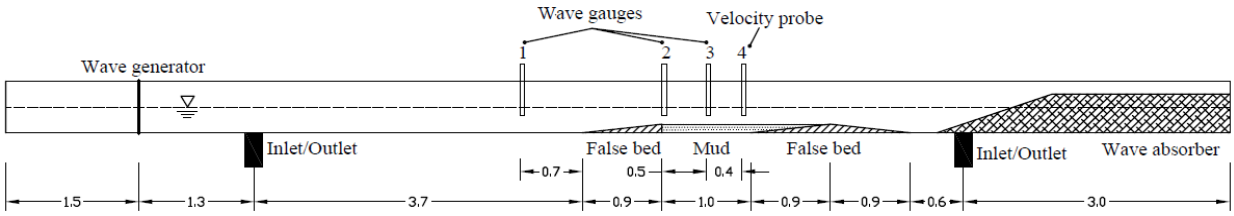

Fig. 1. Sketch of experimental setup, units in meters

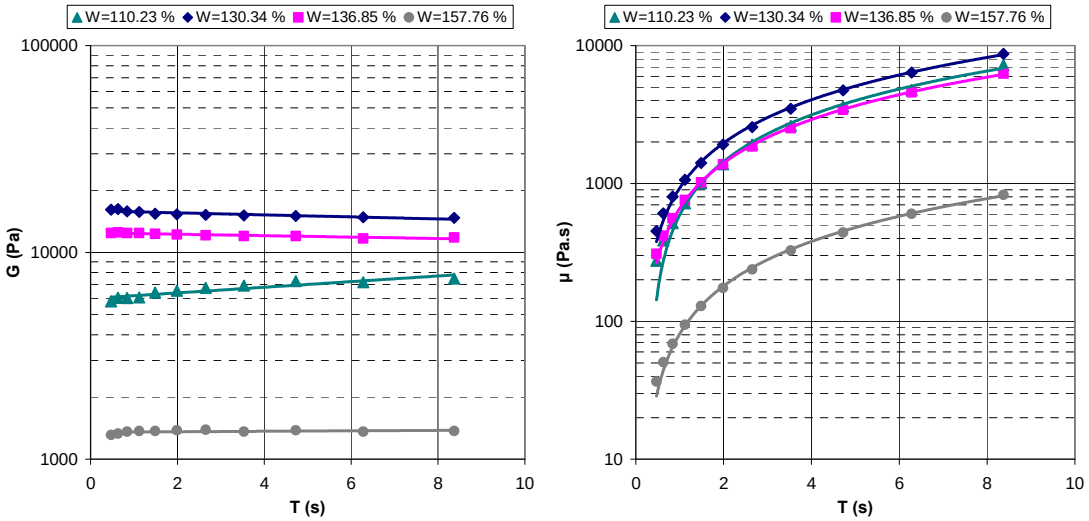

Fig. 2. Elastic modulus and dynamic viscosity of used kaolinite

Table 1. Relationship of viscoelastic parameters of kaolinite versus period and water content ratio

W=110.23 %	$G = 5986.8\ e^{0.0314T}$	$\mu = 850.98T - 258.77$
W=130.34 %	$G = 15898\ e^{-0.0113T}$	$\mu = 1040.7T - 112.75$
W=136.85 %	$G = 12447\ e^{-0.008T}$	$\mu = 749.81T - 88.453$
W=157.76 %	$G = 1351.8\ e^{0.0025T}$	$\mu = 99.504T - 18.281$

Regular monochromatic waves and irregular waves of JONSWAP and Bretschneider spectra with following, opposing, and no current conditions were examined. Table 2 presents the measured wave characteristics, current velocities and calculated wave height attenuation rates assuming an exponential wave height decay. H_{m0}, H_{mean}, and T_m stand for significant wave height by spectral calculation ($H_{m0} = 4\sqrt{m_0}$), mean wave height ($H_{mean} = \sqrt{2\pi m_0}$) and spectral mean wave period, respectively. The plus and minus signs of velocities indicate following and opposing currents, respectively.

RESULTS AND DISCUSSIONS

As an example, Fig. 3 shows the measured Bretschneider wave spectra at gauge No. 2 (beginning of mud section) with following, opposing, and no current conditions. Because of short duration of wave action of about 60-90 seconds, the spectral shape has not been completely developed. The discrepancy is mainly attributed to the flap-type wavemaker that is not capable to exactly generate the same input

Table 2. Measured wave characteristics and current velocities of test runs

Wave spectrum	Test No.	Rep. wave	Wave height (cm)		Wave period T_m (s)		k_i (1/m)	U (cm/s)	W (%)
			Gauge 2	Gauge 3	Gauge 2	Gauge 3			
Bretschneider	BTN1	H_{m0}	3.564	3.409	0.831	0.850	0.08938	-10.32	126.15
		H_{mean}	2.203	2.127			0.06993		
	BTN2	H_{m0}	2.748	2.728	0.801	0.795	0.01459	0	125
		H_{mean}	1.698	1.656			0.04975		
	BTN3	H_{m0}	2.848	2.784	0.802	0.798	0.04538	+9.2	129.5
		H_{mean}	1.711	1.687			0.02800		
	BTN4	H_{m0}	4.906	4.678	0.842	0.848	0.09505	-9.84	135.71
		H_{mean}	2.974	2.952			0.01472		
	BTN5	H_{m0}	3.942	3.780	0.797	0.792	0.08345	0	127.9
		H_{mean}	2.462	2.385			0.06291		
	BTN6	H_{m0}	3.301	3.253	0.824	0.812	0.02967	+9.9	128.4
		H_{mean}	1.983	1.950			0.03404		
JONSWAP	JTN7	H_{m0}	4.710	4.361	0.801	0.814	0.15388	-9.21	130.56
		H_{mean}	2.789	2.669			0.08784		
	JTN8	H_{m0}	4.391	3.951	0.798	0.800	0.21108	0	133.97
		H_{mean}	2.615	2.372			0.19519		
	JTN9	H_{m0}	3.922	3.723	0.815	0.800	0.10452	+9.47	137.65
		H_{mean}	2.376	2.199			0.15468		
	JTN10	H_{m0}	3.398	3.182	0.803	0.815	0.13101	-9.62	137.5
		H_{mean}	2.034	1.959			0.07500		
	JTN11	H_{m0}	3.112	2.941	0.822	0.815	0.11292	0	135.71
		H_{mean}	1.800	1.776			0.02640		
	JTN12	H_{m0}	2.672	2.610	0.830	0.829	0.04657	+9.96	133.33
		H_{mean}	1.569	1.535			0.04464		
Regular	RTN13	H_{m0}	4.910	4.469	0.781	0.784	0.18819	-9.85	126.44
		H_{mean}	4.754	4.354			0.17542		
	RTN14	H_{m0}	4.937	4.471	0.792	0.790	0.19794	0	135.09
		H_{mean}	4.840	4.411			0.18523		
	RTN15	H_{m0}	4.022	3.776	0.773	0.783	0.12604	+9.61	129.67
		H_{mean}	3.886	3.666			0.11684		
	RTN16	H_{m0}	3.577	3.325	0.794	0.794	0.14651	-10.43	136.67
		H_{mean}	3.508	3.287			0.12981		
	RTN17	H_{m0}	3.170	2.999	0.795	0.796	0.11058	0	133.33
		H_{mean}	3.133	2.959			0.11437		
	RTN18	H_{m0}	2.711	2.684	0.785	0.791	0.02055	+9.62	133.27
		H_{mean}	2.626	2.614			0.00897		

incident waves for all three conditions (i.e. opposing, following and no current). When similar incident waves are applied, the wave energy increases due to an opposing current and decreases with the presence of a following current.

Two run tests of measured incident wave spectra at gauge No. 2 and attenuated wave spectra at gauge No. 3 are illustrated in Fig. 4. It is noted that because of the short length of mud section, the difference of the wave spectra at two wave gauges is small. The wave spectral deformation due to current effect is calculated based on the theory of Huang et al. (1972). In order to simulate the energy dissipation on mud layer, the deformed wave spectra due to current at the beginning of mud section is discretized to a number of harmonic regular waves (Zhang and Zhao, 1999). The attenuated wave spectra is then calculated by the numerical model of Soltanpour et al. (2007).

Table 3 shows the representative wave parameters of the measured and simulated wave spectra due to current action at gauge No. 2. It is assumed that the generated input wave spectra for the conditions of opposing and following currents are both similar to no current condition.

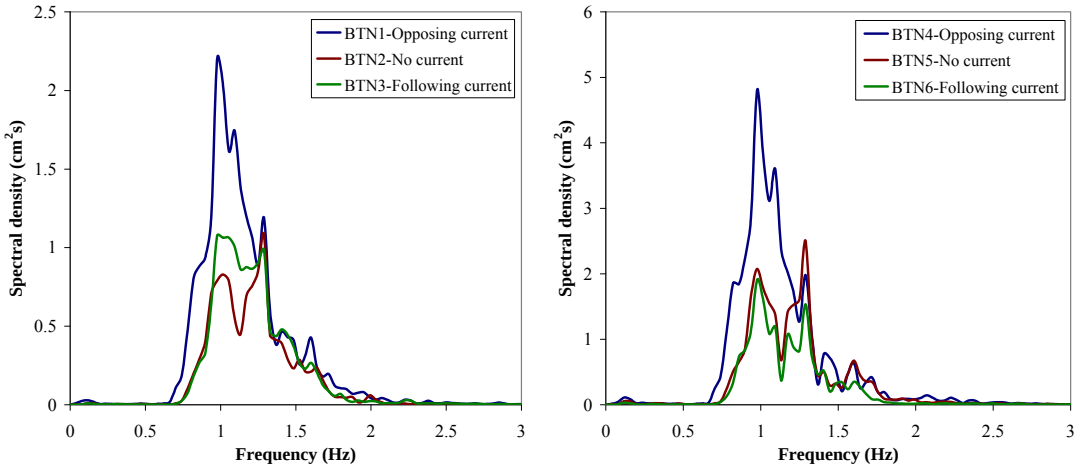

Fig. 3. The measured wave spectra in gauge No. 2 with opposing, following, and no current conditions

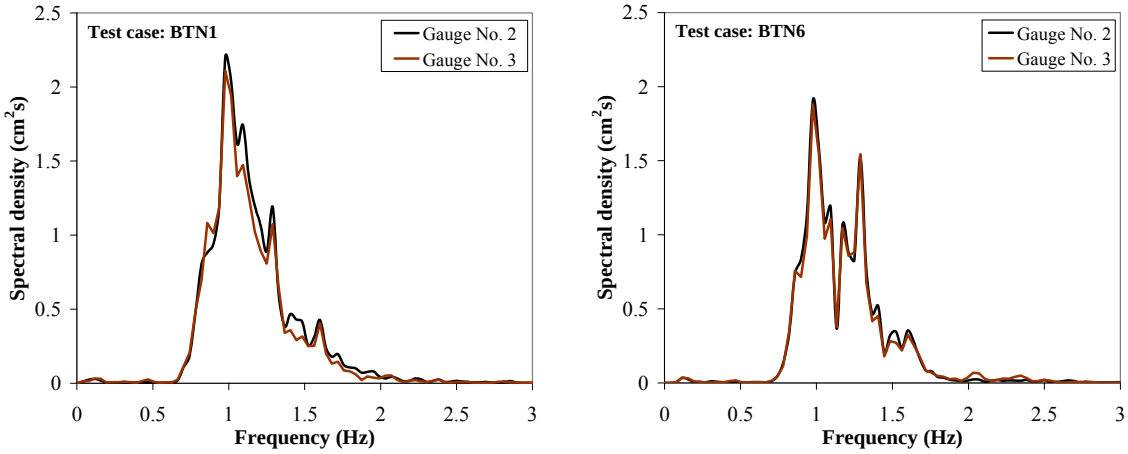

Fig. 4. Sample cases of measured wave spectra before and on the muddy bed

Table 3. Comparisons of measured and calculated waves at gauge 2

Test No.	*U* (cm/s)	Measured wave (cm)		Transformed wave (cm)	
		H_{m0}	H_{mean}	H_{m0}	H_{mean}
BTN1	-10.32	3.564	2.203	3.326	2.083
BTN3	+9.2	2.848	1.711	2.412	1.511
BTN4	-9.84	4.906	2.974	4.767	2.987
BTN6	+9.9	3.301	1.883	3.470	2.174

However, as it was mentioned before, it was not possible to generate the same incident wave conditions in three comparable runs, i.e. opposing, following and no current conditions, because of the flap-type wavemaker.

In order to investigate the attenuation of the deformed wave spectra due to muddy bed, the dissipation of irregular wave on mud section was modeled. Fig. 5 shows the comparison of the measured and simulated wave spectra at gauge 3. The corresponding representative wave parameters obtained from the attenuated wave spectra are also listed in Table 4. The graphical and tabulated comparisons indicate that the irregular attenuated waves can be predicted by numerical model.

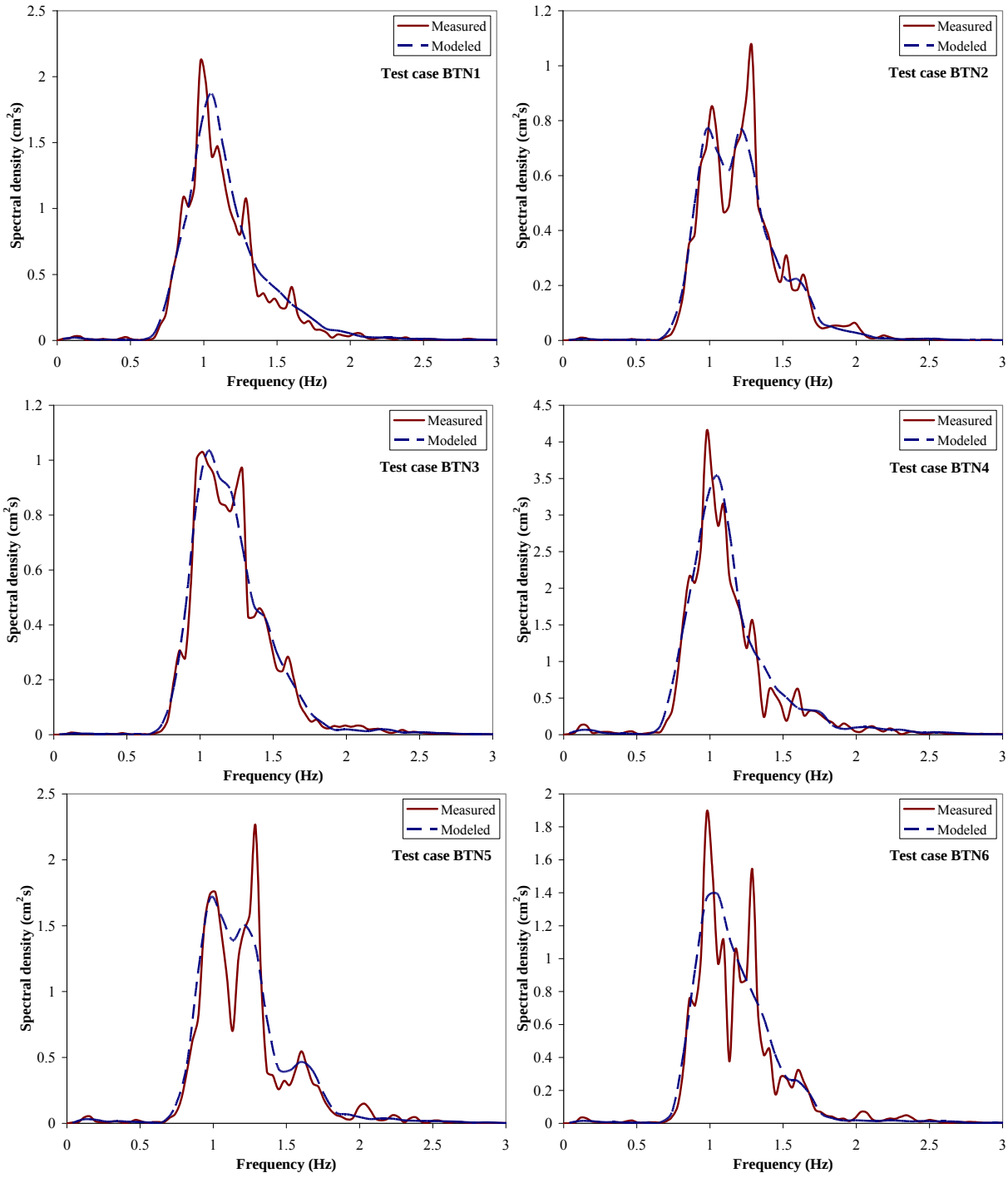

Fig. 5. Comparison of measured and calculated wave spectra on muddy bed

SUMMARY AND CONCLUSIONS

The irregular wave interaction with opposing and following currents and the spectral changes of waves passing over a muddy bed are studied throughout a series of wave flume experiments. It is revealed that the exponential decay is a good estimation for regular and irregular wave heights attenuation over muddy beds. Both approaches of representative and spectral wave analyses were used in numerical modeling showing acceptable agreements with laboratory data. In general, wave energy increases due to an opposing current and it decreases in the presence of a following current. Furthermore, the dissipation of both regular and irregular waves along the mud can be approximated by the exponential decay.

Table 4. Comparison of measured and modeled representative wave heights at gauge 3

Test No.	Modeled wave		Measured wave	
	H_{m0} (cm)	H_{mean} (cm)	H_{m0} (cm)	H_{mean} (cm)
BTN1	3.744	2.345	3.409	2.127
BTN3	2.939	1.841	2.784	1.687
BTN4	5.137	3.218	4.678	2.952
BTN6	3.385	2.121	3.253	1.950

REFERENCES

An, N.N., and T. Shibayama. 1994. Wave-current interaction with mud bed, *Proc. of 24th Coastal Engineering Conference*, ASCE, 2913-2927.

Bretherton, F.P., and C.J.R. Garrett. 1968. Wavetrains in inhomogeneous moving media, *Proc. of the Royal Society,* 302(1471), 529-554.

Brevik, I., and B. Aas. 1980. Flume experiment on waves and currents I. Rippled bed, *Coastal Engineering*, 3, 149-177.

Dalrymple, R.A. 1974. A finite amplitude wave on a linear shear current, *J. Geophysical Research,* 79, 4498-4504.

De Wit P.J. and C. Kranenburg. 1996. On the effects of a liquefied mud bed on wave and flow characteristics, *Journal of Hydraulic Research*, 34:1, 3-18.

Gade, H.G. 1958. Effects of non rigid, impermeable bottom on plane surface wave in shallow water, *J Marine Research*, 16, 61-82.

Huang, N.E., D.T. Chen, and C.C. Tung. 1972. Interactions between steady non-uniform currents and gravity waves with applications for current measurements, *J. Physical Oceanography*, 2, 420-431.

Kaihatu, J.M., and N. Tahvildari. 2012. The combined effect of wave-current interaction and mud-induced damping on nonlinear wave evolution, *Ocean Modelling*, 41, 22–34.

Longuet-Higgins, M.S., and R. W. Stewart. 1961. The changes in amplitude of short gravity waves on steady non-uniform currents, *J. Fluid Mech.*, 10, 529-549.

Peregrine, D.H. 1976. Interaction of water waves and currents, *Advances in Applied Mechanics*, 16, Academic Press, New York, 117 pp.

Soltanpour M., S.A. Haghshenas, and T. Shibayama. 2008. An integrated wave-mud-current interaction model, *31st Coastal Eng. Conf., ASCE*, Hamburg, Germany, 2852-2861.

Soltanpour, M., T. Shibayama, and Y. Masuya. 2007. Irregular wave attenuation and mud mass transport, *Coastal Eng. Journal*, 49, 127-148.

Thomas, G.P. 1981. Wave-current interactions: an experimental and numerical study, Part 1 linear waves. *J. Fluid Mech.* 110, 457-474.

Whitham, G.B. 1962. Mass, momentum and energy flux in water waves, *J. Fluid Mech.*, 12, 135-147.

Zhang Q.H. and Z.D. Zhao. 1999. Wave-mud interaction: wave attenuation and mud mass transport, *Proc. of Coastal Sediments,* 99, 1867-1880.

Zhao, Z.D. and H.Q. Li. 1994. Viscous damping of irregular wave propagation over mud seabeds, *Proc. of International Conference in Hydro-Technical Engineering for Port and Harbor Construction*, 1291-1300.

Zhao, Z.D., J.J. Lian, and J.Z. Shi. 2006. Interactions among waves, current, and mud: numerical and laboratory studies, *Advances in Water Resources*, 29, 1731–1744.